SPECTROSCOPIC IMAGING OF CORE-SHELL STRUCTURED PT-CO NANOPARTICLES BY ABERRATION-CORRECTED STEM

By:
Randi Cabezas

In Conjunction with:
Julia A. Mundy, Huolin L. Xin, Vic Liu, Junliang Zhang,
Rohit Makharia, and Frederick T. Wagner

Mentor:
Dr. David A. Muller

Department of Electrical and Computer Engineering,
Florida International University
Department of Applied Physics and Engineering,
Cornell University
General Motors Fuel Cell Research Laboratory
2009

To: Dr. E. George Simms, Director

      This Undergraduate Research Report in Applied Physics and Engineering, written by Randi Cabezas, entitled "**Spectroscopic Imaging of Core-Shell Structured Pt-Co Nanoparticles by Aberration-Corrected STEM**" is submitted to you in partial fulfillment of the requirements for the Ronald E. McNair Post Baccalaureate Achievement Program. The McNair associate director and the candidate's research supervisor have read this report. We recommend that it be approved.

Dr. David A. Muller
Associate Professor,
Cornell University

Dr. J. Scott Hamilton
Associate Director McNair Program
Florida International University

This report by **Randi Cabezas** is approved.

Dr. E. George Simms
Director McNair Program
Florida International University

<div align="center">

McNair's Scholar's Program
Florida International University
2009

</div>

Abstract

One of the key challenges in developing hydrogen fuel cells as an effective means of energy storage and/or generation for automobile applications is improving the catalysis of the oxygen reduction reaction (ORR). Recent studies have found that replacing pure platinum with a platinum 3d-metal alloy can increase the catalytic activity. Here, the nanoscale structure of Pt_3Co –shown to produce the highest catalyst activity -- was investigated. By using STEM and EELS the atomic distribution of platinum and cobalt within nanoparticles was analyzed for heat-treated particles, heat-treated and subsequent acid leaching, and particles that were used in a fuel cell. It was found that heat treatment leaves platinum-rich regions along the {111} facets. Subsequent acid-leaching causes the dissolution of cobalt from the outer structure, creating a core-shell structure composed of a Pt-rich shell and a Pt-Co core where the shell thickness is independent terminating facet orientation. No cobalt was detected in the particles that were cycled 30,000 times in a fuel cell.

TABLE OF CONTENT

List of Figures

List of Acronyms and Symbols

Å	Angstroms
ADF	annular dark field image
BF	bright field image
Co	cobalt
DM	Digital Micrograph
EDX	Energy Dispersive X-ray Spectroscopy
EELS	Electron Energy Loss Spectroscopy
eV	electron volt
FFT	Fast Fourier Transform
GM	General Motors Company
HAADF	high angle annular dark field image
MCR	Multivariate Curve Resolution
nm	nanometers
ORR	oxygen reduction reaction
PEM	proton exchange membrane
Pt	platinum
px	pixel
RG	red-green image
STEM	Scanning Transmission Electron Microscope
TEM	Transmission Electron Microscope

Introduction

In today's world, it has become an important priority to identify potential clean fuel sources or alternative methods of powering vehicles. One such method is the use of fuel cells.

Fuel cells are electrochemical devices. These devices produce energy from the combination of a fuel and an oxidant in the presence of a catalyst. The main focus herein is on a particular type of fuel cell design called the Proton Exchange Membrane (PEM). A typical PEM design uses hydrogen gas as a fuel and oxygen (usually from air) as an oxidant. The PEM operations are fundamentally divided into two stages: the first stage of the process takes place in the anode of the fuel cell where the hydrogen gas gets separated into protons and electrons in the presence of a catalyst. The protons are allowed to go through the proton-exchange membrane, while the electrons are forced to go outside of the fuel cell to perform a task, i.e. turning chemical energy into electrical energy. The second stage of the operation occurs in the cathode of the fuel cell where recombination of protons and electrons occurs once the electrons reach the cathode. The protons and electrons recombine in presence of the catalyst (usually pure platinum) and the oxidant (figure 1). This particular combination is desirable since it generates benign byproducts, water and heat. This system provides for the conversion of energy as an environmentally safe and noise-free process.
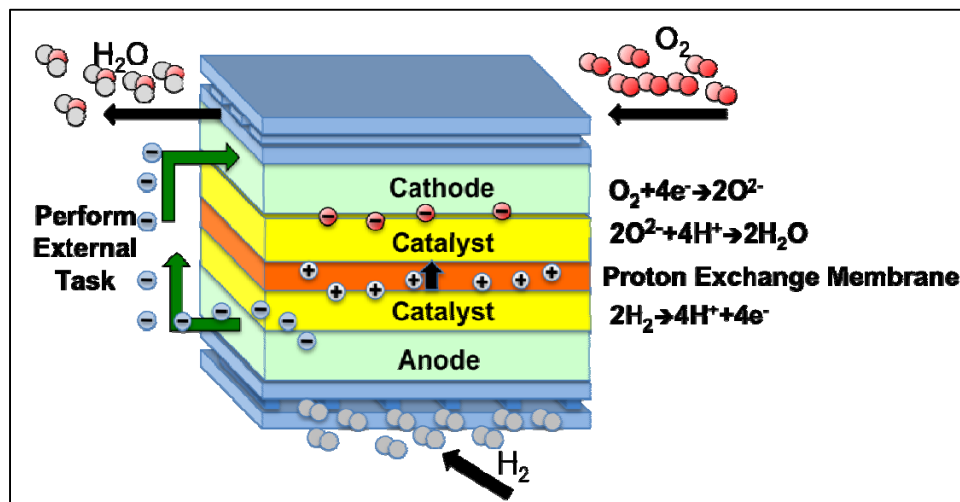
Figure 1*. Diagram of a Proton Exchange Membrane fuel cell design.*

Hydrogen Fuel is introduced into the anode where it is split into protons and electrons. The electrons are forced to go outside of the fuel cell to perform an external task while the protons are allowed to go through the proton exchange membrane. Recombination of protons and electrons with an oxidant takes place in the cathode in presence of a pure platinum catalyst, producing water as a byproduct. (Mundy et al., 2009)

However, fuel cells do not have widespread automotive applications due to two main limitations. First, the materials used in the construction of the fuel cells make the cost of fabrication and operation particularly high at \$107/kW in 2006 (Garland, 2007). Second, the durability and long-term performance of the fuel cells are not up to par with industry standards. Both of these issues can be related to the use of pure platinum as a catalyst. Platinum is an expensive transition metal, accounting for more than 80% of the cost for a fuel cell stack (Garland, 2007). Not only that, but studies have shown that the presence of platinum, and hence performance of the fuel cell, decreases dramatically as the life of the fuel cells is extended (Shao-Horn et al., 2007; Stamenkovic et al. 2004 and 2006; Nørskov et al. 2004; Wagner 2009).

In order to improve the fuel cell's performance substantial studies have been conducted. These studies have shown that combining pure platinum with secondary metals have increased the amount of platinum that remains catalytically active as the life of the fuel cell is extended and thus the active use of the fuel cell. The highest ranking of these 3d-metal alloys was a combination of platinum and cobalt (Stamenkovic et al., 2007). Pt_3Co nanoparticles were shown to produce a ten-fold increase in catalytic activity (Stamenkovic et al., 2007). These nanoparticles are the interest and focus of our research.

When platinum (Pt) and cobalt (Co) are alloyed to form nanoparticles, it was widely predicted that a core-shell structure was formed with an outer shell of Pt surrounding a Pt-Co core (Xu et al., 2004). The purpose of this work is to investigate this core-shell geometry in more depth; in particular, to identify the effect of different treatments on this fragile structure.

This study is focused in analyzing the effect of three different treatments on Pt-Co nanoparticles. These treatments are heat treatment, heat treatment and acid leaching, and particles that were used in a fuel cell. It is hypothesized that by heat-treating the Pt and Co would diffuse and return, or remain uniformly distributed throughout the particle. If that is the case acid leaching should dissolve the outer layers of the nanoparticles. Understanding the microscopic details of this structure will bring us one step closer to effectively identify the optimal catalyst material.

This study will be done using scanning transmission electron microscopy and electron energy loss spectroscopy. In STEM an incident beam of electrons is focused into a small point, approximately 1Å, and then scanned across the sample (Muller et al.,

2008). By collecting scattered electrons at every point in the sample, images are formed. Furthermore, by combing STEM with EELS a chemical composition map of a given sample can be formed. EELS uses inelastically scattered electrons --electrons that have lost energy as they penetrate through the sample-- to produce a spectrum of energy loss. Once this spectrum is compared with a known spectrum a detailed compositional map can be extracted.

Materials, Equipment and Method

Materials

General Motor Co., a collaborator for this project, provided three different platinum cobalt nanoparticles. The three nanoparticles were: heat-treated, heat-treated and acid leached and 30,000 cycled particles. The heat-treated particles consisted of commercially available particles that have been heated at 800°C for 6 hours. Heat-treated and Acid Leached particles are heat-treated particles that have been placed in 1M HNO_3, nitric acid, for 48 hours. The 30,000 cycled particles consisted of particles that had been used in a fuel cell. These particles underwent 30,000 voltage cycles, i.e. turned on and off, to simulate the use of a car for approximately five years. Due to lack of time, the emphasis of this research was the heat-treated and heat-treated and acid leached particles. Each of the samples mentioned above were provided as a crushed powder. As such the best way of preparing them for analysis was to use a pestle and mortar technique. In this technique the sample is dissolved in a solvent (ethanol in this case) and further crushed using a pestle and mortar; then placed the liquid solution into carbon and copper TEM grids.

Equipment

The Pt-Co nanoparticles were imaged and characterized using a Nion UltraSTEM 100KeV fifth-order aberration-corrected scanning transmission electron microscope (α_{max}=33 mrads). This machine is capable of both high spatial resolution (~1Å) and high beam current (150-200pA) for electron energy loss spectroscopy (Muller et al., 2008). In addition, a 120KeV Tecnai™ T-12 transmission electron microscope (TEM) was used with an EDAX x-ray spectrometer in order to perform energy dispersive x-ray spectroscopy (EDX). Several software packages were used including Gatan's Digital Micrograph™ (DM) version 3.11 and Mathwork's 2008b MATLAB®.

Method

The following procedure was used to analyze all the data acquired. First and foremost, the samples were placed in the microscope and imaged using the bright field (BF) and annular dark field (ADF) detectors. In addition, spectroscopic images were taken in which an EELS spectrum was collected at each pixel on an approximately 64 by 64 pixel map. Due to the high usable beam current unique to the NION UltraSTEM over other 5th order aberration corrected microscopes, a typical map could be collected on timescales in which sample damage and drift concerns are minimal. The sample was imaged before and after the spectrum image acquisition to ensure that there was no radiation damage incurred to the sample during the data collection. A spectral map could be collected to readily show the Co signal in less than 10 minutes; the weaker Pt signal could monitored after a 40 minute acquisition. A sample spectrum showing both Pt and Co signal is shown on figure 2.
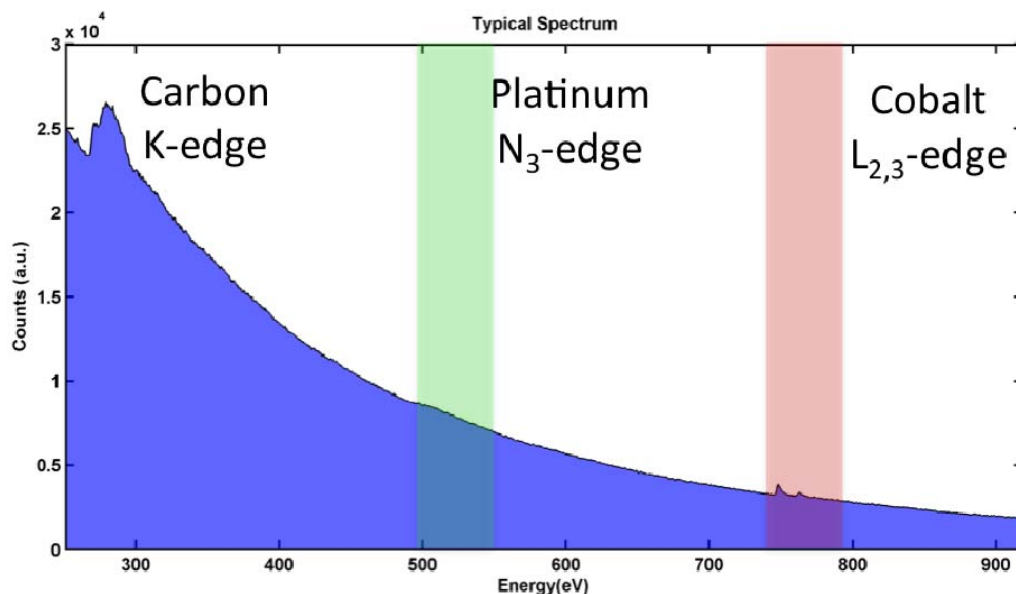
Figure 2. *Sample EELS Spectrum.*

Sample EELS Spectrum for Pt-Co nanoparticles, this spectrum was produced by taking a line profile across one of the particles, (averaging 64 px). Nanoparticles are sitting on the Carbon TEM grid, hence the Carbon K-edge at approximately 290eV. Both the Pt N_3-edge and the Cobalt $L_{2,3}$-edge can be seen clearly at approximately 515eV and 780eV respectively.

An FFT of the HAADF or ADF image was taken in order to see the diffractogram using DM. The diffractogram contains information about lattice parameters. The spacing and direction between reflected spots was compared to known spacing; using a calculated lattice constant of 3.82Å (Wagner, 2009). In this manner the different crystallographic particle terminating facets [111], [110] and [100] were indexed. Figure 3a, shows a sample ADF image with a diffractogram inset.
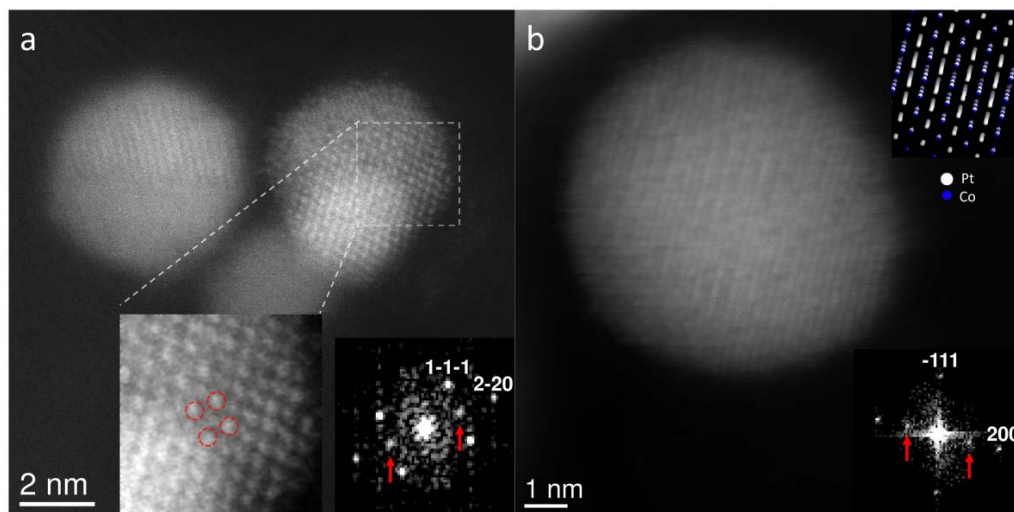
Figure 3. *ADF-STEM images of selected Pt-Co nanoparticles.*

(a) The red circles in the left inset mark the pure Pt column in the Pt_3Co $L_{1,2}$ ordered structure along the [110] zone axis. The right inset is the diffractogram of the particle. The red arrows point to the super-lattice spots expected from the ordered structure; (b) a particle with ordered structure tilted off the [0-11] axis. A schematic of the lattice is shown in the upper inset. (Mundy et al., 2009)

Using EELS data in DM, individual platinum and cobalt composition maps were extracted. Due to a low signal to noise ratio in these maps, mostly platinum maps, different background subtraction techniques were implemented which removed the residual carbon from the data. After experimenting with a variety of methods, it was found that for a Co signal the best background subtraction consisted of first extracting a complete spectrum of our data using DM's standard power law background subtraction with two forced regions. The result of this was a second spectral map with a largely insignificant carbon component. A second background subtraction technique was used, this time using DM's standard linear background subtraction to remove the residual carbon left. The signal was then extracted producing a pure cobalt map. For the platinum signal, it was best to perform a Multivariate Curve Resolution (MCR) fit using two

components. This background subtraction was performed in MATLAB. This method provided significant improvement in the signal to noise ratio of the Pt signal.

Once the individual components were extracted then line profiles were obtained across the indexed direction for the Co, Pt and ADF images using DM's live profile tool. These line profiles were originally averaged over a distance of 10 pixels across; it was later found that an average of 3 pixels allowed the index to be selected without sacrificing signal to noise ratio. The line profiles were drawn across the Pt and Co maps in order to obtain the signal width for each map; in addition, line profiles on the ADF images were drawn to quantify the particle size. It is important to note that the line profiles were obtained in identical directions for all three of these images.

Once the line profiles were extracted they were fitted in MATLAB using custom scripts (see the appendix). The scripts implemented the following fit:

$$y = a * \frac{erf(b*(x-c)) + erfc(d*(x-(c+e))) - 1}{2}$$

This equation uses an error function and a complementary error function to fit the data. In the equation parameters "a", "b" and "d" are stretching parameters while "c" provides the center of the error function and "c+e" specifies the center of the complementary error function, thus "e" represents the distance between both functions center. In this manner the width of the particle expressed in the line profile can be quantified by looking at parameter "e". This width is expressed in pixel and converted to actual unit of length, nanometers, using the conversion factors from the DM files. This process was repeated for every particle in our analysis. Figure 4 shows a typical line profile and error curve fit.
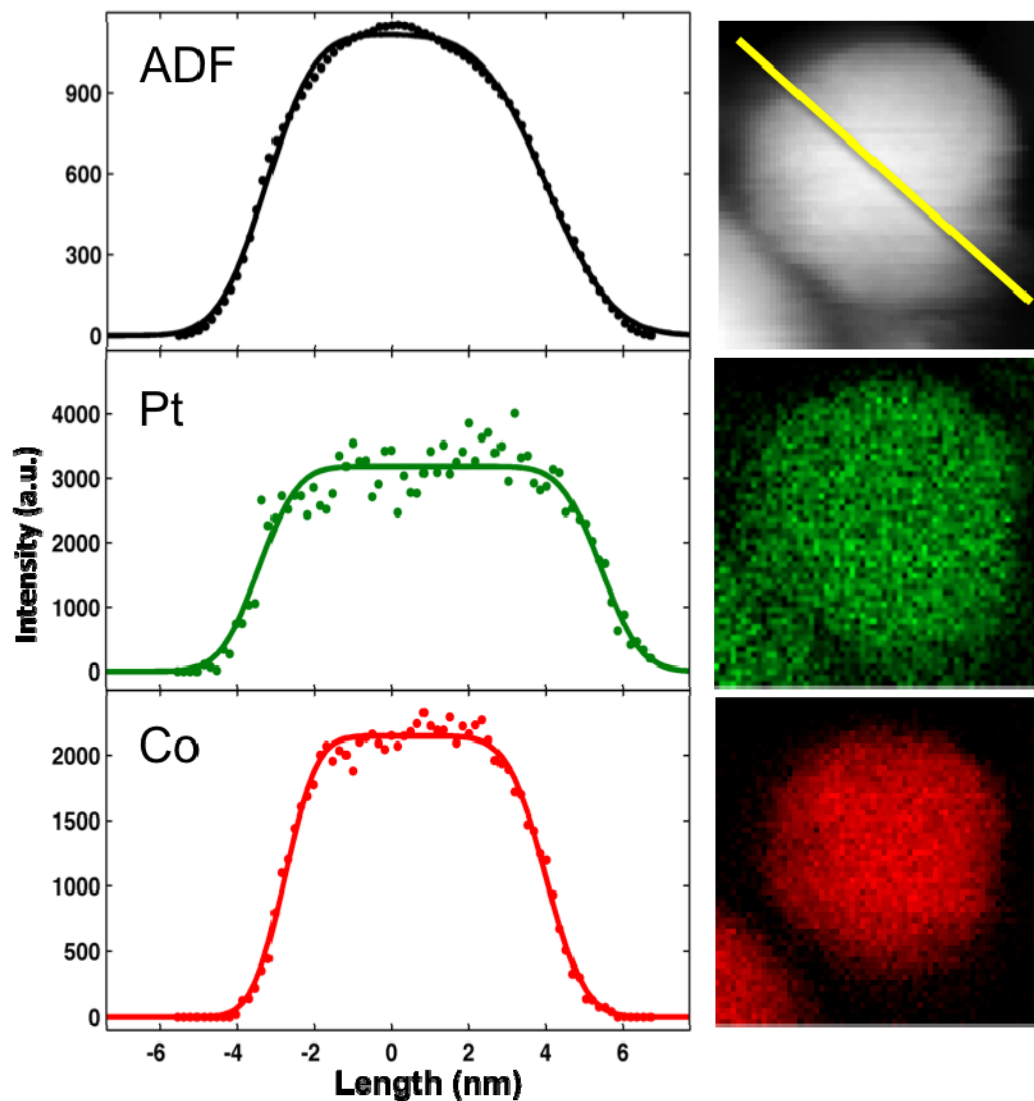
Figure 4. *Sample Line Profile and Error Curve Fit.*
Image shows the corresponding ADF-STEM image, Pt and Co composition map and the corresponding error curve fit for each one. The shown platinum signal was background subtracted in DM and not using MCR. The MCR fits greatly improved the signal to noise ratio for this particle.

In the case of a difference between the widths of Pt and Co signal, as shown on figure 4, the difference was calculated and divided by two. This measurement is the shell thickness.

Results

By understanding the microscopic details of the Pt-Co nanoparticles a better catalyst will be produced for use in fuel cells. As previously mentioned, different treatments should cause different changes in the nanoparticles' structures. What follows are detailed results divided by treatments.

Heat-treated

The heat-treated sample consisted of commercially available particles that were heated to 800°C for 6 hours. The purpose of this was to restore the particles to near pristine conditions, since details of the commercial particles were not provided. Figure 4a, shows a typical acquisition for the heat-treated particles. While looking at the combined RG image one can see that both Pt and Co are dispersed throughout the particle which suggest that the concentration of both platinum and cobalt is similar; except for the Pt-rich (green) region on the upper left portion of the particle. After performing quantitative analysis, it was concluded that the Pt-rich regions found on the heat-treated particles corresponded to {111} facet terminated regions. This facet contains a weak Pt-rich region with thickness of 1.6±0.5Å. In comparison the {100} facet does not show the existence of a platinum terminated region; the thickness for the {100} facets was 0.6±0.7Å.
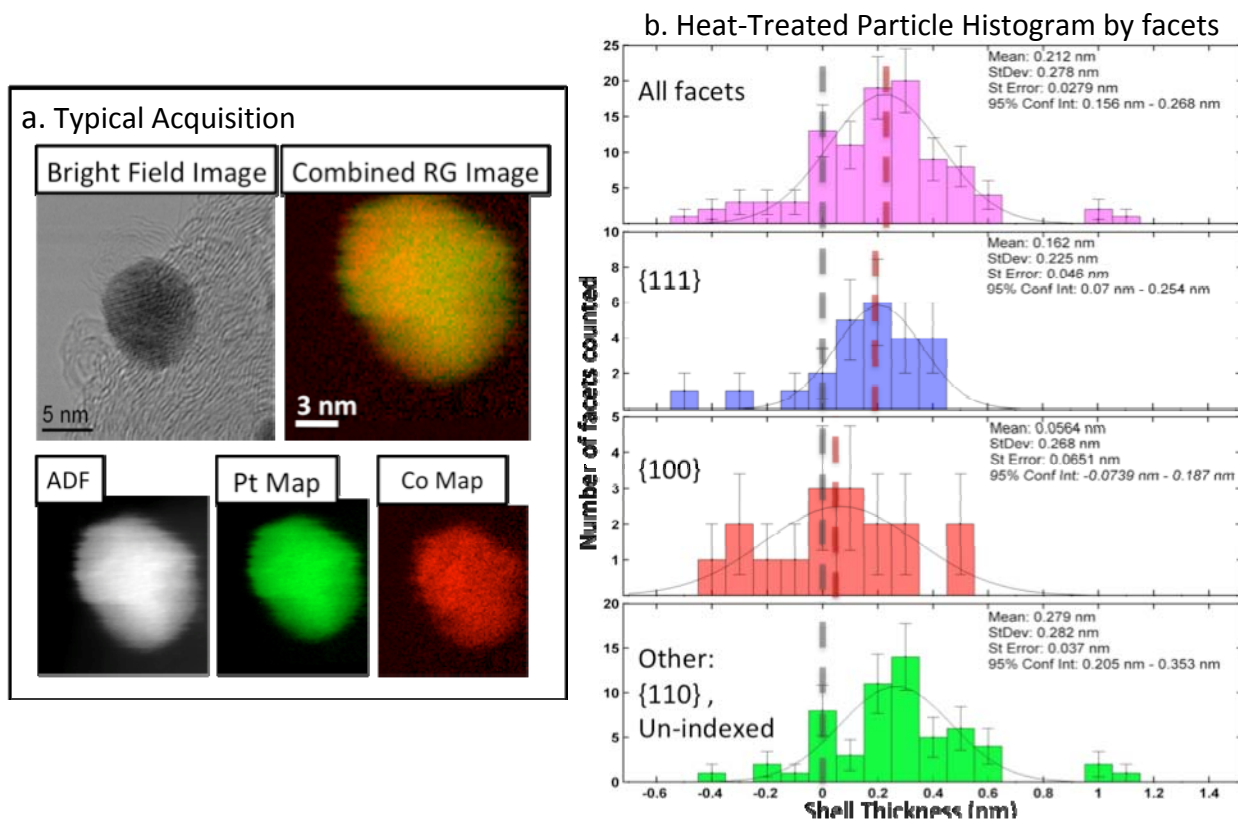
Figure 5. *Heat-Treated Particles Summary.*

(a) Typical acquisition for a heat-treated particle, showing bright field image, ADF-STEM image, both Pt and Co compositional map, and the combined RG image. In the RG image a Pt-rich region can be seen on the top left of the particle. (b) Shell Thickness Histogram separated by terminating facet; with a red dashed line passing through the mean of each data. Pt-rich regions along the {111} facets but not the {100} facets.

Heat-treated and Acid-Leached

The heat-treated and acid leached particles consisted of heat-treated particles that were also placed in nitric acid for 48 hours. Figure 6 shows a selected particle from the heat-treated and acid leached sample. This image was chosen since it shows a clear representation of a thick Pt-rich shell surrounding a Pt-Co core. This is accentuated in the chemical composition maps shown in fig 6a. While looking at the Pt map one can clearly

see that the Pt signals of the upper and lower particles are clearly overlapping; if one were to look at the Co map one sees that these two signals do not overlap. The Co map is confined to its particular core in the center of each particle. From the histograms shown in fig. 6b the presence of a thick Pt shell, thickness of 6±0.3Å is clearly seen. Furthermore, unlike the heat-treated particles there is no statistical dependence of shell thickness on terminating facets. In this case both {100} and {111} facets have similar shell thickness.
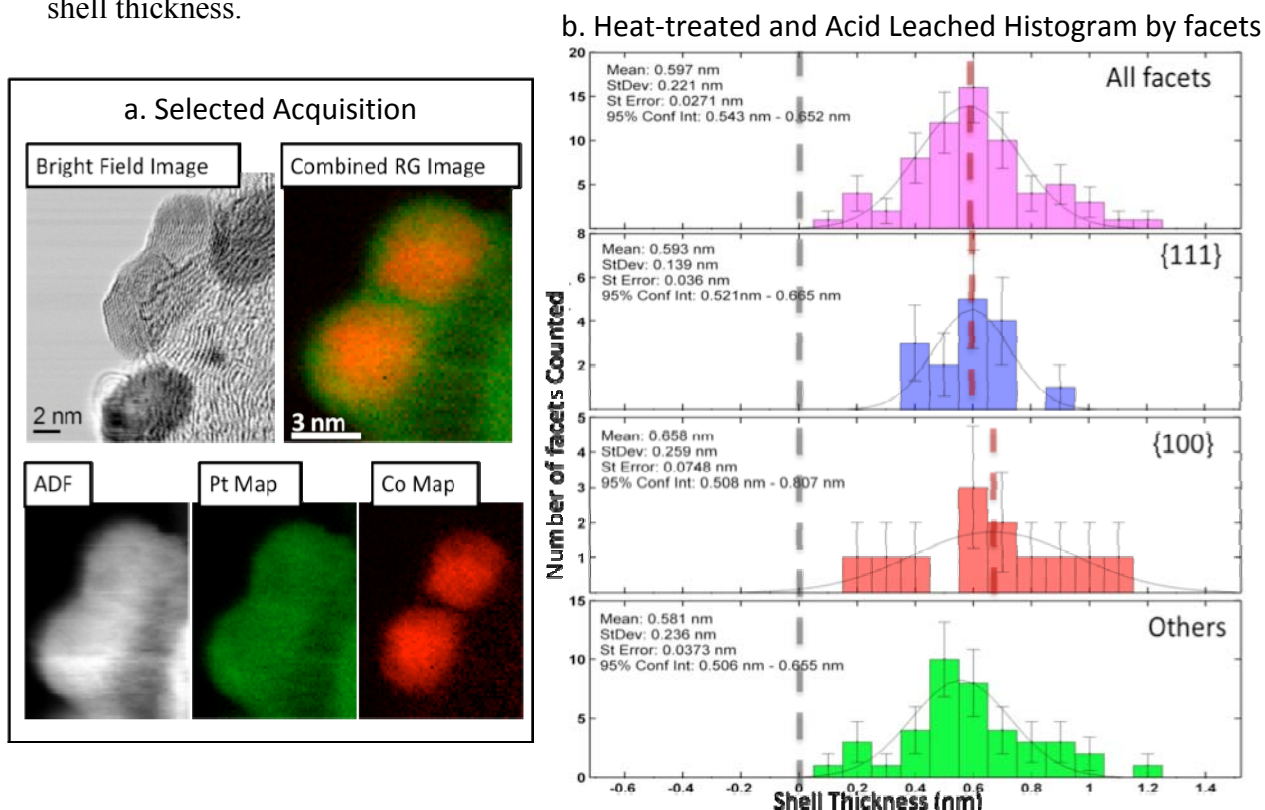
Figure 6. Heat-treated and Acid Leach Particles Summary.

(a) Selected acquisition showing the bright field image, the ADF-STEM image, the Pt and Co compositional maps and the combined RG image. This image demonstrates the existence of a core-shell structure; while the Pt signals of neighboring particles touch, the corresponding Co signal does not. (b) Shell Thickness Histogram separated by terminating facet; with a red dashed line passing through the mean of each data. No statistically significant dependence of shell thickness on terminating facet.

30,000 Cycled

The 30,000 cycled particles consisted of sample nanoparticles that had been voltage cycled in a fuel cell. The emphasis of the research project was on the heat-treated and heat-treated and acid leached samples. As such, the 30,000 cycled samples were only briefly analyzed. The EELS spectrum depicted on figure 7, showed the presence of Pt and the lack of Co. Since no Co signal was detected the Co composition map was blank and the RG image would be the same as the Pt map.
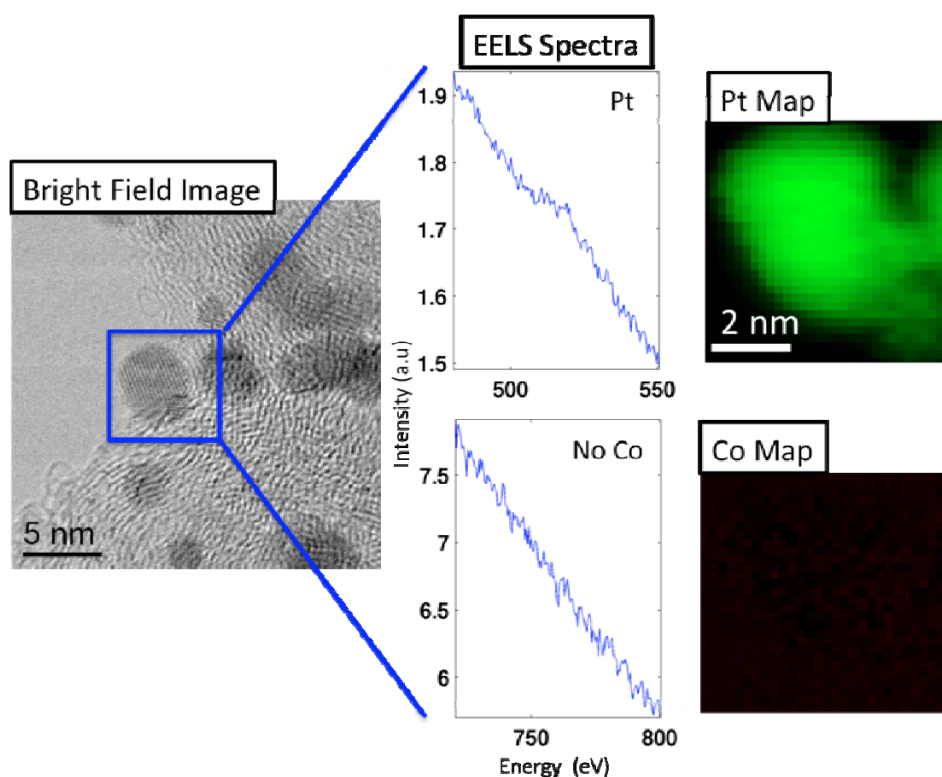
Figure 7. 30,000 Cycled Particle Summary.

The EELS spectrum shows that there is no cobalt component. As a result, the cobalt map is empty and the RG image will only consist of Pt. (Mundy et al. 2009)

In order to verify the validity of this result a second spectroscopic measurement was performed. Energy Dispersive X-ray Spectroscopy (EDX) was performed. A sample EDX spectrum is shown in figure 8. The top spectrum corresponds to a heat-treated and acid leached sample, while the bottom sample corresponds to the 30,000 cycled samples. When comparing the two, it is clear that no cobalt was detected in the 30,000 cycled particles. It is important to note that the carbon peak (low energy peak) and the copper peak correspond to the TEM grid and are not part of the samples.
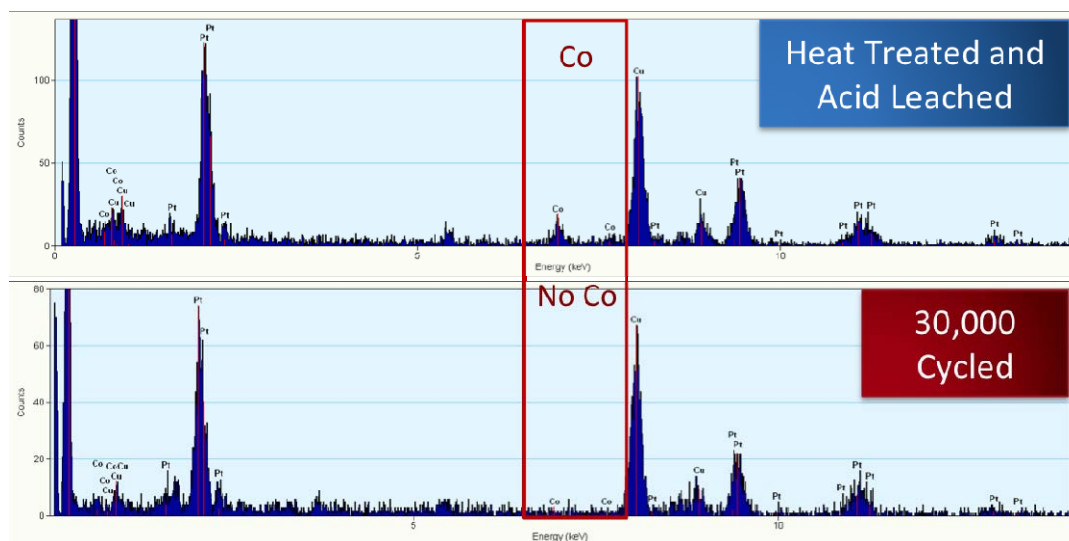
Figure 8. 30,000 Cycled EDX Spectrum.

The above spectrum further shows that no Co was detected for the 30,000 cycled samples. The spectrum shown above corresponds to a heat-treated and acid leached particle, it is shown for comparison purposes.

Discussions

Pt$_3$Co is a primary candidate for catalyst material in automobile fuel cell applications. This alloy has been shown to provide substantial improvement in the fuel cell's performance. However, this improvement is not well understood. This study seeks to understand how different treatments affect the microscopic structure of these valuable nanoparticles.

As shown in the results section, there are clear distinctions between the heat-treated samples and the heat-treated and acid leached samples, namely, the existence of a complete Pt shell surrounding a Pt-Co core in the latter and only Pt-rich regions in the former. While similar results have been imaged before for comparable nanoparticles, this is the first instance that they are seen and quantified solely based on chemical composition maps.

The heat-treated particles showed Pt-rich regions along the {111} facets. These regions had a thickness of 1.6±0.5Å. Most importantly, there existed a statistically significant difference of shell thickness on terminating facets, which agreed with previous calculations (Hu Y., et al 2004). It was found that there was a distinct difference on shell thickness based on terminating facet. Pt-Co nanoparticles along {111} facets could cause an improvement on catalytic activity similar to the ten-fold improvement shown for Pt-Ni on facet {111} over any other terminating facet (Stamenkovic et al., 2007).

Heat-treated and acid leached samples contained a core-shell structure. This structure consisted of Pt-rich shell surrounding a Pt-Co core, with a shell thickness of 6±0.3Å and no statistical significance on terminating facet. This particular treatment is the preferred treatment for utilization in fuel cells, since it places the catalytically active

element, platinum, on the outside of the nanoparticles where it can easily interact with the reactants in the fuel cell and thus increase ORR activity (Wagner, 2009). However, the fuel cell itself consists of an acidic environment; the above result suggests that further cobalt will continue to leach out. Thus yield a partial or complete dissolution of alloying metal. This result is consistent with previous studies conducted by our collaborators at GM (Wagner, 2009).

The limited amount of 30,000 cycled particles analyzed in this study showed the lack of alloying metal, cobalt. This result was unexpected since some cobalt has been previously found in similar samples (Wagner, 2009). It is possible that the amount of cobalt present is below detection limit of the equipment used. Furthermore, it is important to note, that our sample size for this particular treatment might not be representative of the population. Further investigating is needed.

Conclusions

In summary, fuel cells are an alternative method of powering automotives in the future. However, they need to be made more economically feasible and reliable in order to be used for practical applications. Both of these issues can be accomplished by finding a more suitable catalyst material. Pt_3Co could be a potential such candidate. From previous research it is known that forming a platinum-cobalt alloy will decrease the cost of production and increase the fuel cell's performance. This research project has brought us one step closer in understanding this important alloy. By using STEM and EELS, it was demonstrated how the structure of this platinum-cobalt alloy changes after various treatments. Namely, it was found that heat-treating a sample restores the particles to a

near-pristine condition in which both Pt and Co are dispersed through the particle. However, after heat treatment some nanoparticles showed relatively small Pt-rich regions along the {111} facets; with a dependence on terminating facet. It was also found that acid leaching of these particles dissolves the outer layers of cobalt, producing a core-shell structure having a Pt shell and Pt-Co core with shell thickness showing no dependence on terminating facets.

Acknowledgments

References

Garland, Nancy. "DOE Fuel Cell Sub-Program". *Fuel Cell Seminar*.Presentation. San

Antonio, Texas. 16-19 October 2007.

Muller, D. A., Fitting Kourkoutis, L., Murfitt, M., Song, J. H., Hwang, H. Y., Silcox, J.,

Dellby, N. & Krivanek, O. L. "Atomic-Scale Chemical Imaging of Composition

and Bonding by Aberration-Corrected Microscopy." *Science* 319, 1073-1076. 2008.

Mundy, J. A., Xin, H. L., Cabezas, R., Muller, D. A., Liu, V., Zhang, J., Makharia, R. &

Wagner, F. T. "Spectroscopic Imaging of Core-Shell Structured Pt-Co

Nanoparticles by Aberration-Corrected STEM." *2009 Microscopy and

Microanalysis Conference*. Poster Presentation. Richmond, VA. 26-30 July 2009.

Nørskov, J. K., Rossmeisl, J., Logadottir, A., Lindqvist, L., Kitchin, J. R., Bligaard, T. &

Johnson, H. "Origin of the Overpotential for Oxygen Reduction at a Fuel-Cell

Cathode." *The Journal of Physical Chemistry B,* 108(46), 17886-17892. 22

October 2004. DOI: 10.1021/jp047349j

Shao-Horn, Y., Sheng, W. C., Chen, S., Ferreira, P. J., Holby, E. F. & Morgan, D.

"Instability of Supported Platinum Nanoparticles in Low-Temperature Fuel Cells."

Springer Science and Business Media 46,285-305. 27 November 2007.

DOI:10.1007/s11244-007-9000-0.

Stamenkovic, V. R., Fowler, B., Mun, B. S., Wang, G., Ross, P. N., Lucas, C. A. &

Markovic, N. M. "Improved Oxygen Reduction Activity on $Pt_3Ni(111)$ via

Increased Surface Site Availability." *Science* 315(5811), 493-497. 26 January 2007.

DOI:10.1126/science.1135941

Stamenkovic, V. R., Mun, B. S., Arenz, M., Mayrhofer, K. J. J., Lucas, C. A., Wang, G., Ross, P. N. & Markovic, N. M. "Trends in electrocatalysis on extended and nanoscale Pt-bimetallic alloy surfaces." *Nature Materials*6, 241-247. 2007. DOI:10.1038/nmat1840.

Stamenkovic, V., Mun, B. S., Mayrhofer, K. J. J., Ross, P. N., Markovic, N. M., Rossmeisl, J., Greeley, J. & Nørskov, J. K. "Changing the Activity of Electrocatalysts for Oxygen Reduction by Tuning the Surface Electronic Structure." *Angewandte Chemie International Edition*, 45(18), 2897-2901. 5 April 2006. DOI:10.1002/anie.200504386

Wagner, F. T. "Automotive Challenges and Opportunities in Oxygen Reduction Electrocatalysts." *Fuel Cell Research Lab, General Motors R&D*. Presentation. Honeoye Falls, NY. 22 July 2009.

Xu, Y., Ruban, A. V., & Mavrikakis, M. "Absorption and Dissociation of O_2 on Pt-Co and Pt-Fe Alloys." *Journal of the American Chemical Society*126(14), 4717-4725. 20 March 2004. DOI: 10.1021/ja031701+.

Appendix: Error Curve Fit Script

The Error Curve Fit was the MATLAB script used to perform the fit to the line profiles extracted from DM. It contains several dependencies, which are explained at the end of the script

```matlab
%Randi Cabezas, Muller Group, 2009 CNS REU, Cornell University
%The purpose of this script is to perform a two-sided error function curve
%fit to the data present in the text file loaded in the 7th line.
%if the ADF data is passed to this function, it will automatically remove
%the background noise

%Dependency "myerf.m" and "findpoints_efn" needs to be in the same directory!
%flag values
%    -1 initial
%     1 find absolute max or min
%     2 manual max or min
%     3 Huolin's service function
%     4 Skipped

z=getfile;

z=char(z);
len=size(z);

fid = fopen('coeficients.txt', 'wt');


for i=1:1:len

    y=load(z(i,:));
    x=1:1:length(y);
%figure; plot(x,y,'o')

    pos=strfind(z(1,:),'\');
    name=z(i,(max(pos)+1):length(z(i,:)));
    name=strrep(name,'.txt','')
    flag=-1; %initializes flag to -1
%Sets all negative numbers to zeros
for j=1:1:length(y)
if y(j)<=0
        y(j)=0;
end
end
%figure; plot(x,y,'o')

%Removes the background and positions the data at zero
if strfind(z(i,:),'ADF')>0 |strfind(z(i,:),'adf')>0
        mm=(y(1)-y(length(y)))/(1-length(y));
        yremove=mm.*x+y(1);
        y2=y-yremove;
        y=y2;
```

```matlab
        display('ADF Background substraction performed for figure:')
        disp(name)
        clear y2yremovemm
end
%figure; plot(x,y,'o')

if i==1
        fprintf(fid, '\n\t NAME\t A\t B\t C\t D\t E\t Left Low Pt\t
Right Low Pt\t Flag \t R^2');
end

    fprintf(fid, '\n %d\t %s\t',i, name);


%++++++++++++++++Getting Initial Conditions++++++++++++++++++++++
points=conv(y,[1 1 1 1 1 1 1 -2 -2 -2 -2 -2 -2 -2 1 1 1 1 1 1 1 ]);
%Conv adds 20 extra points
points=points(11:length(y)+10);

%figure; plot(points)
points1=points(1:round(length(points)/2));
points2=points(round(length(points)/2)+1:length(points));
%figure; plot(points1)
%figure; plot(points2)
flag=1;
ll_pt=round(find(points1==max(points1)));
lh_pt=round(find(points1==min(points1)));
rl_pt=round(find(points2==max(points2))+length(points)/2);
rh_pt=round(find(points2==min(points2))+length(points)/2);

%clear points1 points2 j

% Previous methods of finding mins and max, the new method works
slightly
% better. Thanks Huolin
%However, when the data is noisy (i.e, Pt) then the second derivative is
%not as effective
%Find max on points from the left
if ll_pt>=lh_pt | rh_pt>=rl_pt
    temp2=-10e10; clear temp1
for i=1:1:length(points)/2
        temp1=points(i);

if temp1>=temp2
            temp2=temp1;
end

if temp2>temp1
            flag=2;
break
end
end
    ll_pt=find(points==temp2);


%Find max on points from the right
    temp2=-1e10;
for i=length(points):-1:length(points)/2
        temp1=points(i);

if temp1>temp2
```

```matlab
                temp2=temp1;
    end

    if temp2>temp1
                flag=2;
break
end
end
    rl_pt=find(points==temp2);
    clear itemp1temp2;

%Find min on points from the left(not exact but provides good initial
%guess)
    temp2=1e6;
for i=ll_pt:1:length(points)/2
        temp1=points(i);

    if temp1<temp2
                temp2=temp1;
end
    if temp2<temp1
                flag=2;
break
end
end
    lh_pt=find(points==temp2);

%Find min on points from the right(not exact but provides good initial
%guess)
    temp2=1e6;
for i=rl_pt:-1:length(points)/2
        temp1=points(i);
    if temp1<temp2
                temp2=temp1;
end
    if temp2<temp1
                flag=2;
break
end
end
    rh_pt=find(points==temp2,1,'last');
end

if length(ll_pt)~=1
    ll_pt=ll_pt(length(ll_pt));
end
%Secondary function in case that the ll_pt and lh_pt are too close
%Coded by Huolin Xin
if (lh_pt-ll_pt)<=3 |(rl_pt-rh_pt)<=3 | y(ll_pt)==y(lh_pt)
|y(rl_pt)==y(rh_pt)
    [ll_pt lh_pt rh_pt rl_pt] = findpoints_efn(x,y,.1,.7);
    flag=3;
end
%If all else fails, user can manually adjust these values to adjust
initial%conditions
%ll_pt=5;
%lh_pt=9;
%rl_pt=51;
%rh_pt=100;

%Calculates/Estimates Initial values
```

```matlab
a_ini=y(lh_pt);
b_ini=3/(2*abs(ll_pt-lh_pt));
c_ini=mean([ll_pt, lh_pt]);
d_ini=3/abs(rl_pt-rh_pt);
e_ini=mean([(rh_pt-lh_pt) (rl_pt-ll_pt)]);

%Allows shift of the values in either direction
initial_conditions =  [a_ini, b_ini, c_ini, d_ini, e_ini];
lower_bound = [a_ini*0.25, b_ini*.25, c_ini*0.25, d_ini*0.25,ll_pt];
%define the lower bound
upper_bound =[a_ini*2, b_ini*2, c_ini*2, d_ini*2, rl_pt]; %define the
upper bound

%checks for errors in the bounds
for k=1:5
if lower_bound(k)==Inf |lower_bound(k)==-Inf |upper_bound(k)==Inf |
upper_bound(k)==Inf| upper_bound(k)==lower_bound(k)
display('Skipping Fit, bounds are either Infinite or the same');
        flag=4;
break
end
end




%skips the particle
if flag==4
        fprintf(fid, 'Skipped, bounds are either Inf or the same');
continue
end


clear a_inib_inic_inid_inie_ini
%++++++++++++++++++++++++++++++++++++++++++++++++++++++++++++++++++++++++++
+++
% WARNING "Maximum number of function evaluations exceeded; increase
options.MaxFunEvals"
%The above can be fixed by this
%configure the optimset for use with lsqcurvefit
%increase the number of function evaluations for more accuracy
options = optimset('lsqcurvefit');
options.MaxFunEvals = 500;

%uses matlab build-in function to do the fit.
[new_parameters,sserror] = lsqcurvefit(@myerf,
initial_conditions,x,y,lower_bound,upper_bound,options);

%Plots Data and Curve Fit
figure; plot(x,y,'o')
h=gcf;
xlabel('Thickness (nm)')
ylabel('Counts (a.u.)')

title(strcat(name,'_Error_Curve_Fit'),'interpreter','none')
hold
x2=-10:1:length(y)+10;
y_fit = myerf(new_parameters,x2);
plot(x2,y_fit,'r')
plotvertline(new_parameters(3),gca,'m');
plotvertline(new_parameters(3)+new_parameters(5),gca,'m');
```

```matlab
    plotvertline(length(x)/2,gca,'y');
    plotvertline(ll_pt,gca,'g');
    plotvertline(rl_pt,gca,'g');

    %R^2 calculations
    ymean=mean(y);
    for i=1:1:length(y)
        sstemp(i)=(y(i)-ymean)^2;
    end
    sstotal=sum(sstemp);
    disp('R squared value:')
    r_squared=1-sserror/sstotal;
    disp(r_squared)
    sterror=sprintf('R-squared: %1.6g',r_squared);
        xlimit = get(gca,'xlim');
        ylimit = get(gca,'ylim');
    text( xlimit(2)*.6,ylimit(2)*.8,sterror);

    fprintf(fid, '%6f\t', new_parameters);
    fprintf(fid, '%6f\t %6f\t %6f\t %6f\t', ll_pt,rl_pt, flag, r_squared);

    %Creates png file of the fit with the same name of size 100 px closes
    the
    %open figure
        outputfigure(name,200)
    %close(h)
    end

    fclose(fid);
```

Dependencies

getfile – a graphical way, open dialog, that allows the user to select the data.

findpoints_efn – an additional method of finding the corner points.

plotvertline – plots a vertical line.

Outputfigure – creates a png file of the current plot.

Note: none of these functions are crucial for the script to work, they were all

implemented to allow batch processing of data.

myerf - contains the equation that will be fitted. This function is crucial, and the above

script will not work without it.

```
function output= myerf(param,x)
a = param(1); %scaling factor
b = param(2); %scaling factor
c=  param(3); %center of the rising leg
d=  param(4); %scaling factor
e=  param(5);   %width

output = a*(-1+(erf(b*(x-c))+erfc(d*(x-c-e))))/2;
```